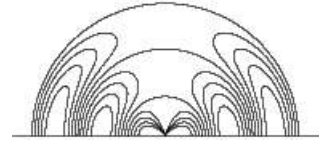


PIERS

Progress In Electromagnetics Research Symposium

PIERS 2018 in Toyama, Japan, 1-4 August, 2018

[PIERS Home](#) | [The EM Academy](#) | [Who's Who in Electromagnetics](#) | [PIERS Online](#) | [Login](#)

Quick Links

[PIERS Guidelines](#)
[Paper Submission](#)
[Session Organization](#)
[Registration](#)
[Locale&Hotel](#)
[PIERS Exhibition](#)
[PIERS Shortcourse](#)
[PIERS Gallery](#)
[PIERS2018 Organization](#)
[PIERS2018 Sponsors](#)
[Author Login](#)
[Reviewer Login](#)

*We are speaking the same language, Maxwell's Equations.
 --- In memory of [Jin Au Kong](#)*

The 40th PIERS in Toyama, JAPAN

1 - 4 August 2018 (From Wednesday to Saturday)



Venue: [Toyama International Conference Center](#) and [ANA Crowne Plaza Toyama](#)

PIERS 2018 Sponsors



Recent PIERS

PIERS2019 in Rome

[PIERS2018 in Toyama](#)
[PIERS2017 in Singapore](#)
[PIERS2017 in St. Petersburg](#)
[PIERS2016 in Shanghai](#)
[PIERS2015 in Prague](#)
[PIERS2014 in Guangzhou](#)
[PIERS2013 in Stockholm](#)
[PIERS2013 in Taipei](#)
[PIERS2012 in Moscow](#)
[PIERS2012 in Kuala Lumpur](#)
[PIERS2011 in Suzhou](#)
[PIERS2011 in Marrakesh](#)
[PIERS2010 in Cambridge](#)
[PIERS2010 in Xi'an](#)
[PIERS2009 in Moscow](#)
[PIERS2009 in Beijing](#)
[PIERS2008 in Cambridge](#)
[PIERS2008 in Hangzhou](#)
[PIERS2007 in Prague](#)
[PIERS2007 in Beijing](#)
[PIERS2006 in Tokyo](#)
[PIERS2006 in Cambridge](#)
[PIERS2005 in Hangzhou](#)
[PIERS2004 in Pisa](#)
[PIERS2004 in Nanjing](#)

.....

Important Dates

- **1 April, 2018**--- Extended Deadline of Abstract Submission [\[Submit\]](#) [\[Guidelines\]](#)
- **1 May, 2018**--- Pre-registration Deadline [\[Login First\]](#) [\[Instruction\]](#)
- **5 May, 2018** --- Extended Paper Submission Deadline [\[Submit\]](#) [\[Guidelines\]](#)
- **1 June, 2018** --- Preliminary Program available
- **15 June, 2018** --- Advance Program available
- **1 July, 2018** --- [Final Program is available now](#) [\[PDF\]](#)

PIERS 2018 Toyama Program

- [Final Program](#) is available now. [\[download PDF version of final printed program\]](#)
- [Proceedings \(extended papers only\)](#) have been published on [IEEE Xplore](#). [\[PDF\]](#)
- [Welcome Message by PIERS 2018 Toyama General Chair](#) is now available.
- **Install PIERS App into your mobile** - [Installation Instructions](#)
- **Program at a Glance**
Please visit [here](#) at the local website, where the Program at a Glance is posted. You can easily have an idea about the entire program by taking a look at this webpage.
- **Opening Ceremony**
Date and time: 16:00-16:40, Wednesday, August 1, 2018
Venue: Toyama International Conference Center
Please visit [here](#) for the [program of the Opening Ceremony](#).
- **Symposium Banquet**
Date and Time: 19:00-21:30, Friday, August 3, 2018
Venue: ANA Crowne Plaza Toyama
Please visit [here](#) for the [program of the Symposium Banquet](#).
- **General Lectures**
During PIERS 2018 Toyama, four General Lectures (GLs) by leading scientists in the electromagnetics community will be scheduled as plenary sessions. There are no other sessions running in parallel to these GLs, and all the PIERS 2018 Toyama participants are invited to join the GLs. Please visit the [GL program at this webpage](#).
- **Pre-Conference Workshop**
Prior to the Conference, a Workshop will be held on July 31, 2018, and all the registered PIERS 2018 Toyama participants are invited to attend the Workshop without extra fees nor advance reservation. Please plan on attending this Workshop! Please visit the [Workshop schedule at this webpage](#).
- **Toyama City Fireworks Festival**
The Toyama City Fireworks Festival will be held 19:45-20:30, August 1, 2018, right after the Symposium Reception. Please get out of the venue and enjoy Toyama's great summer event! Fireworks festivals held in Toyama in the past can be seen [from this website](#).

PIERS 2018 Toyama

Progress In Electromagnetics Research Symposium

Program

August 1–4, 2018
Toyama, JAPAN

www.emacademy.org
www.piers.org

PIERS 2018 TOYAMA TECHNICAL PROGRAM

Session 1A1

FocusSession.SC5: Remote Sensing for Hydrological Applications 1

Wednesday AM, August 1, 2018

Room T1

Organized by Jian-Cheng Shi, Hui Lu

Chaired by Jian-Cheng Shi, Hui Lu

08:30 Fully Coherent Model for Layered Bicontinuous
KeynoteMedium Using Analytical Method of Feynman Dia-
gram for Applications in Microwave Remote Sensing
of Snow Cover

Jiyue Zhu (University of Michigan); Leung Tsang (University of Michigan); Shurun Tan (University of Michigan); Son V. Nghiem (California Institute of Technology);

09:00 Improving Snow Fraction Spatio-temporal Continuity
Invited Using a Combination of MODIS and Fengyun-2 Satel-
lites over China

Lingmei Jiang (Beijing Normal University); GongXue Wang (Beijing Normal University); Jian-Cheng Shi (Institute of Remote Sensing Applications, Chinese Academy of Sciences);

09:20 Time-series Passive Microwave Observations Applied
Invited for Snow Estimation

Jinmei Pan (Institute of Remote Sensing and Digital Earth, Chinese Academy of Science); Chuan Xiong (Institute of Remote Sensing and Digital Earth, Chinese Academy of Sciences); Jian-Cheng Shi (Institute of Remote Sensing Applications, Chinese Academy of Sciences); Deyuan Geng (Institute of Remote Sensing and Digital Earth, Chinese Academy of Science); Haokui Xu (University of Michigan);

09:40 Time-series Ground Based X and Ku Band SAR Ob-
Invited servation of Seasonal Snow: Modeling and Retrieval
Chuan Xiong (Institute of Remote Sensing and Digital Earth, Chinese Academy of Sciences); Jiancheng Shi (Institute of Remote Sensing and Digital Earth, CAS); Jinmei Pan (Institute of Remote Sensing and Digital Earth, Chinese Academy of Science); Haokui Xu (Institute of Remote Sensing and Digital Earth, Chinese Academy of Science); Tianjie Zhao (Institute of Remote Sensing and Digital Earth, Chinese Academy of Science); Deyuan Geng (Institute of Remote Sensing and Digital Earth, Chinese Academy of Science);

10:00 Measurement and Modeling of Multi-frequency Mi-
Invited crowave Emission of Soil Freezing and Thawing Pro-
cesses

Tianjie Zhao (Jointly Sponsored by Institute of Remote Sensing and Digital Earth, Chinese Academy of Sciences); Jian-Cheng Shi (Institute of Remote Sensing Applications, Chinese Academy of Sciences); Shaojie Zhao (Beijing Normal University); Kun-Shan Chen (Institute of Remote Sensing and Digital Earth, Chinese Academy of Sciences); Pingkai Wang (Institute of Remote Sensing and Digital Earth, Chinese Academy of Sciences); Shangnan Li (Institute of Remote Sensing and Digital Earth, Chinese Academy of Sciences); Chuan Xiong (Institute of Remote Sensing and Digital Earth, Chinese Academy of Sciences); Qing Xiao (Institute of Remote Sensing and Digital Earth, Chinese Academy of Sciences);

10:20 Z-R Relationships for Weather Radar in Indonesia
from the Particle Size and Velocity (Parsivel) Opti-
cal Disdrometer

Marzuki (Andalas University); Hiroyuki Hashiguchi (Kyoto University); Mutya Vonnisa (Andalas University); Harmadi (Andalas University); Muzirwan (National Institute of Aeronautics and Space); Sugeng Nugroho (Indonesian Agency for Meteorological, Climatological and Geophysics); Meri Yoseva (Andalas University);

10:40 **Coffee Break**

- 16:40 Validating SMAP SSS with in Situ Data and Process Oriented Analysis
Wenqing Tang (California Institute of Technology); Simon H. Yueh (California Institute of Technology); Alexander G. Fore (California Institute of Technology); Akiko Hayashi (California Institute of Technology);
- 17:00 Accurate Surface Fields and Emissivities in Ocean Scattering and Emission Using Neighborhood Impedance Boundary Condition (NIBC) with Dense Grid in Surface Integral Equations
Yanlei Du (Institute of Remote Sensing and Digital Earth, Chinese Academy of Sciences); Tai Qiao (University of Michigan); Leung Tsang (University of Michigan); Xiao Feng Yang (Institute of Remote Sensing and Digital Earth, Chinese Academy of Sciences);

Session 3P1b
SC5: Inverse Scattering 1

Friday PM, August 3, 2018

Room T1

Organized by Motoyuki Sato, Toshifumi Moriyama

Chaired by Motoyuki Sato, Toshifumi Moriyama

- 17:20 Adaptive Array Radar Imaging of Moving Human Body for Measurement of Vital Signs
Takuya Sakamoto (University of Hyogo); Kentaro Konishi (University of Hyogo); Masashi Muragaki (Kyoto University); Shigeaki Okumura (Kyoto University); Toru Sato (Kyoto University);
- 17:40 Accuracy Enhanced Distorted Born Iterative Method with Envelope Based Boundary Extraction for Microwave Mammography
Shouhei Kidera (The University of Electro-Communications); Kazuki Noritake (The University of Electro-Communications);
- 18:00 Development of Microwave CT Mammography Device
Yoshio Nagayama (Nihon University); Tomoya Hanashima (Nihon University); Tomohiko Asai (Nihon University); Soichiro Yamaguchi (Nihon University); Toshifumi Moriyama (Nagasaki University); Toshiyuki Tanaka (Nagasaki University); Hayato Tsuchiya (Nihon University);

Session 3P2a
FocusSession.SC5: SAR Imaging and Applications

Friday PM, August 3, 2018

Room T2

Organized by Kun-Shan Chen, Toshifumi Moriyama

Chaired by Kun-Shan Chen, Toshifumi Moriyama

- 13:00 Compound Scattering Matrix by Dipoles in the Range Invited Direction
Yoshio Yamaguchi (Niigata University); Yoshihiro Yamazaki (Niigata University); Hiroyoshi Yamada (Niigata University);
- 13:20 An Experimental Assessment of Polarimetric L-band Backscattering Using GB-SAR Data
Sevket Demirci (Mersin University); Betul Yilmaz (Mersin University); Serhat Gokkan (Mersin University); Hakan Isiker (Mersin University); Caner Ozdemir (Mersin University);
- 13:40 RCS Characteristics Analysis of Trihedral Corner Reflector for Bistatic SAR Tandem Mode Radiometric Calibration
Qiaona Zheng (Institute of Electronics, Chinese Academy of Sciences); Jun Hong (Institute of Electronics, Chinese Academy of Science); Yu Wang (Institute of Electronics, Chinese Academy of Sciences);
- 14:00 Research on the Sparse Aperture Remote Imaging System Based on the Freeform
Quanying Wu (Suzhou University of Science and Technology); Junliu Fan (Suzhou University of Science and Technology); Baohua Chen (Suzhou University of Science and Technology);
- 14:20 Airborne Single Pass X-band FMCW INSAR Instrument for the Accurate DEM Generation — Principle and Validation
 Invited
Masanobu Shimada (Tokyo Denki University); Akira Nohmi (Alouette Technology); Hitoshi Nohmi (Alouette Technology); Mayumi Noguchi (The Geospatial Information Authority of Japan); Sho Takahashi (The Geospatial Information Authority of Japan);
- 14:40 Integration of Heterogeneous InSAR Measurements Invited for Mapping Complete and Accurate Three-dimensional Surface Displacements: A Case Study of 2016 Mw 7.8 Kaikōura Earthquake, New Zealand
Jun Hu (Central South University); J. H. Liu (Central South University); Lixin Wu (Northeastern University); Zhi-Wei Li (Central South University); Q. Sun (Hunan Normal University);

- 30 Detection of Small and Large Hidden Metallic Objects via Passive Millimeter Wave Imaging System with an Auto-segmentation Routine
Hakan Isiker (Mersin University); Sevket Demirci (Mersin University); Betul Yilmaz (Mersin University); Serhat Gokkan (Mersin University); Caner Ozdemir (Mersin University);
- 31 An Analysis of Relationship between Urban Heat Island in the Tropics in Extremely Hot Days with Land Use Using Landsat 8 Image — A Case Study in Hanoi Vietnam
Nguyen Thanh Hoan (Institute of Geography, Vietnam Academy of Science and Technology); Tran Duy Phien (Institute of Geography, Vietnam Academy of Science and Technology); Dao Dinh Cham (Institute of Geography, Vietnam Academy of Science and Technology);
- 32 Automatic Sport Fields Detection from China GF-1 Satellite Image Data via Improved SSD Model
Zhengchao Chen (Institute of Remote Sensing and Digital Earth, CAS); Kaixuan Lu (Institute of Remote Sensing and Digital Earth, CAS); Xuan Yang (Institute of Remote Sensing and Digital Earth, CAS); Baipeng Li (Institute of Remote Sensing and Digital Earth, Chinese Academy of Sciences); Jianwei Gao (Institute of Remote Sensing and Digital Earth, Chinese Academy of Sciences); Mufeng Yao (Institute of Remote Sensing and Digital Earth, CAS);
- 33 Impact of Usage of Multiple-satellite Sensors on Accuracy of Sea Surface Wind Data
Ayumi Koizumi (Tokai University); Masahisa Kubota (Tokai University); Kunio Kutsuwada (Tokai University);
- 34 Double Weighted Fourier Transform (DWFT) in Statistical Problems
Sergei I. Knizhin (Irkutsk State University); Mikhail V. Tinin (Irkutsk State University);
- 35 Experiment and FDTD Simulation of Antenna for the Microwave CT
Tomoya Hanashima (Nihon University); Yoshio Nagayama (Nihon University); Tomohiko Asai (Nihon University); Toshifumi Moriyama (Nagasaki University); Toshiyuki Tanaka (Nagasaki University); Soichiro Yamaguchi (Nihon University); Hayato Tsuchiya (Nihon University);
- 36 The Method of Adaptive Gaussian Decomposition Based Recognition and Extraction of Scattering Mechanisms
Xinyi He (Science and Technology on Electromagnetic Scattering Laboratory); Pengcheng Gao (Science and Technology on Electromagnetic Scattering Laboratory); Wei Gao (Science and Technology on Electromagnetic Scattering Laboratory); Xiao Lin Mi (Science and Technology on Electromagnetic Scattering Laboratory); Yuan Zhang (Science and Technology on Electromagnetic Scattering Laboratory);
- 37 Using Spectral Residual Method to Identification Buried Objects from GPR B-Scan Image
Yao Qin (Henan University of Technology); Jing Wan (Henan University of Technology); Jieyi Yang (Henan University of Technology); Li Hong Qiao (Henan University of Technology); Chunhua Zhu (Henan University of Technology); Qifu Wang (Henan Academy of Science, Applied Physics Institute Co., Ltd);
- 38 A Novel Encoding and Decoding Method for Packaging Goods Based on Grayscale-Information Matrix
Guo Chun Wan (Tongji University); Wen Jing Liu (Tongji University); Jian Zhou (Tongji University); Mei Song Tong (Tongji University);
- 39 Development of Middle-power W-band Gyrotron in IAP RAS
Mikhail Yu. Glyavin (Federal State Budgetary Scientific Institution “Federal Research Center The Institute of Applied Physics of the Russian Academy of Sciences”); Mikhail D. Proyavin (Institute of Applied Physics of the Russian Academy of Sciences (IAP RAS)); Anton S. Sedov (Federal State Budgetary Scientific Institution “Federal Research Center The Institute of Applied Physics of the Russian Academy of Sciences”); Evgeni S. Semenov (Institute of Applied Physics of the Russian Academy of Sciences); Andrey S. Zuev (Federal Research Center “Institute of Applied Physics RAS”); Alexander I. Tselkov (Federal State Budgetary Scientific Institution “Federal Research Center The Institute of Applied Physics of the Russian Academy of Sciences”);
- 40 Wavelength-dependent Terahertz Wave Modulation in Organic/Si Hybrid Structures
Joong Wook Lee (Chonnam National University);
- 41 Topological Properties and Edge State in Parity-time Symmetrical Waveguide Array
Qi Dong Fu (Shanghai Jiaotong University);

- 14:20 Automatic Building Extraction Based on Deep Convolutional Neural Networks from High-resolution Remote Sensing Images
Jianwei Gao (Institute of Remote Sensing and Digital Earth, Chinese Academy of Sciences); Zhengchao Chen (Institute of Remote Sensing and Digital Earth, CAS); Xuan Yang (Institute of Remote Sensing and Digital Earth, CAS); Qun Ma (Institute of Remote Sensing and Digital Earth, Chinese Academy of Sciences); Baipeng Li (Institute of Remote Sensing and Digital Earth, Chinese Academy of Sciences);
- 14:40 Handheld Bistatic Subsurface Radar Using Accelerometer
Kazutaka Kikuta (Tohoku University); Motoyuki Sato (Tohoku University);
- 15:00 Investigation for the Measurement Accuracies of Silica Waveguide Sidewall Angles with Confocal Laser Scanning Microscope
Hongpeng Shang (Changchun University of Science and Technology); De Gui Sun (Changchun University of Science & Technology; University of Ottawa); Jinzhu Gao (Institute of Metal Research, Chinese Academy of Sciences); Peng Yu (Changchun University of Science & Technology); Qingyu Sun (Changchun University of Science and Technology); Peng Liu (University of Ottawa); Trevor J. Hall (University of Ottawa);
- 15:20 An Experimental Study of Foliage Penetrating Radar with Coherent Change Detection
Sevket Demirci (Mersin University); Betul Yilmaz (Mersin University); Hakan Isiker (Mersin University); Serhat Gokkan (Mersin University); Caner Ozdemir (Mersin University);
- 15:40 **Coffee Break**
- 16:20 Metasurface Design by Surrogate-assisted Optimization
Binbin Zhu (Kuang-Chi Institute of Advanced Technology); Yang Yang (Tsinghua University); Yiqi Liu (Kuang-Chi Institute of Advanced Technology); Xiao Guo (Kuang-Chi Institute of Advanced Technology); Ke Deng (Tsinghua University); Chunlin Ji (Kuang-Chi Institute of Advanced Technology);
- 16:40 Multiphysics Modeling for Ferroelectric Materials
Shigu Cao (Shenzhen Inequation Technology Co. Ltd.);
- 17:00 GL Full Wave Modeling and Ray Tracing Method for Cloak
Jianhua Li (GL Geophysical Laboratory); Lee Xie (GL Geophysical Laboratory); Feng Xie (GL Geophysical Laboratory); Ganquan Xie (GL Geophysical Laboratory);
- 17:20 r Can Be Negative in a New Negative World on Acoustic, EM, and Seismic Modeling and Inversion
Jianhua Li (GL Geophysical Laboratory); Feng Xie (GL Geophysical Laboratory); Lee Xie (GL Geophysical Laboratory); Ganquan Xie (GL Geophysical Laboratory);
- 17:40 A New GLHUANPII-3 Electromagnetic Invisible Cloak
Jianhua Li (GL Geophysical Laboratory); Feng Xie (GL Geophysical Laboratory); Lee Xie (GL Geophysical Laboratory); Ganquan Xie (GL Geophysical Laboratory);

Session 4P2a
SC5: Advances in PolSAR/PolInSAR Analysis and Applications

Saturday PM, August 4, 2018
Room T2

Organized by Hiroyoshi Yamada, Ryoichi Sato
Chaired by Hiroyoshi Yamada, Ryoichi Sato

Session 4P1b
Electromagnetic Modeling and Inversion and Applications

Saturday PM, August 4, 2018
Room T1

Organized by Jianhua Li, Ganquan Xie
Chaired by Shigu Cao, Ganquan Xie

- 16:00 Plane Wave Coupling to Overhead Lines over Stratified Earth
Zeyneb Belganche (Mohammed V University); Abderrahman Maaouni (Mohammed V University); Ahmed Mzerd (Mohammed V University); Ayoub Lahmidi (Universite Mohammed V);

- 13:00 Detection of Landslides of the 2016 Kumamoto Earthquake by Using Two Single-pass Cross-track Interferometry Airborne SAR Data
Toshifumi Moriyama (Nagasaki University); Fumiaki Jitsufuji (Nagasaki University);
- 13:20 Monitoring Permafrost Environments with Polarimetric SAR and Optical Remote Sensing Data
Sang-Eun Park (Sejong University);

[Browse](#)[My Settings](#)[Get Help](#)[Conferences](#) > [2018 Progress in Electromagne...](#)[Back to Results](#)

An Experimental Assessment of Polarimetric L-Band Backscattering Using GB-SAR Data

[<< Results](#)

5 Author(s)

Sevket Demirci ; Betul Yilmaz ; Serhat Gokkan ; Hakan Isker ; Caner Ozd...

[View All Authors](#)

6
Full
Text Views

[Export to](#)[Collabratec](#)

Alerts

[Manage](#)[Content Alerts](#)[Add to Citation](#)[Alerts](#)

More Like This

Polarimetric calibration of X-band airborne synthetic aperture radar using corner reflectors and an active radar calibrator IGARSS '98. Sensing and Managing the Environment. 1998 IEEE International Geoscience and Remote Sensing Symposium Proceedings. (Cat. No.98CH36174)
Published: 1998

Calibration experiments of the CRL/NASDA X/L-band airborne synthetic aperture radar IGARSS'97. 1997 IEEE International Geoscience and Remote Sensing Symposium Proceedings. Remote Sensing - A Scientific Vision for Sustainable Development
Published: 1997

[View More](#)

Abstract

Document Sections

1. Introduction
2. Experimental Scenario
3. Measurement Results
4. Conclusion

[Authors](#)[Figures](#)[References](#)[Keywords](#)[Metrics](#)[More Like This](#)[Downl](#)[PDF](#)

Abstract: The microwave backscattering from a complex environment is subject to numerous factors such as wavelength, viewing geometry, polarization of the transmitted wave and targ... [View more](#)

Metadata

Abstract: The microwave backscattering from a complex environment is subject to numerous factors such as wavelength, viewing geometry, polarization of the transmitted wave and target attributes including roughness, shape, size, orientation and dielectric properties. Therefore, the characteristics and amount of backscatter data varies from case to case. In an effort to better understand this complex mechanism of backscattering from distributed surfaces, the SAR image characteristics of a typical land area are assessed through a readily feasible polarimetric ground-based synthetic aperture radar (GB-SAR) system working at L-band frequencies. Because of their standard use in data calibration, trihedral corner reflectors (TCR) as well as dipole-like objects are also deployed in the measurements to extract their polarimetric GB-SAR image features.

Published in: 2018 Progress in Electromagnetics Research Symposium (PIERS-Toyama)

Date of Conference: 1-4 Aug. 2018

INSPEC Accession Number: 18383930

Date Added to IEEE Xplore: 03 January 2019

DOI: 10.23919/PIERS.2018.8597890

ISBN Information:

Publisher: IEEE

Electronic ISSN: 1559-9450

Conference Location: Toyama, Japan

[Contents](#)

SECTION 1.

Introduction

An Experimental Assessment of Polarimetric L-band Backscattering Using GB-SAR Data

Sevket Demirci¹, Betul Yilmaz¹, Serhat Gokkan²,
Hakan Isiker², and Caner Ozdemir¹

¹Department of Electrical-Electronics Engineering, Mersin University, Çiftlikkoy, Mersin 33343, Turkey

²Vocational School of Technical Sciences, Mersin University, Çiftlikkoy, Mersin 33343, Turkey

Abstract— The microwave backscattering from a complex environment is subject to numerous factors such as wavelength, viewing geometry, polarization of the transmitted wave and target attributes including roughness, shape, size, orientation and dielectric properties. Therefore, the characteristics and amount of backscatter data varies from case to case. In an effort to better understand this complex mechanism of backscattering from distributed surfaces, the SAR image characteristics of a typical land area are assessed through a readily feasible polarimetric ground-based synthetic aperture radar (GB-SAR) system working at L-band frequencies. Because of their standard use in data calibration, trihedral corner reflectors (TCR) as well as dipole-like objects are also deployed in the measurements to extract their polarimetric GB-SAR image features.

1. INTRODUCTION

Synthetic aperture radar (SAR) is an imaging radar with the final aim being to accurate retrieval of targets' physical parameters including shape, size, roughness, orientation, and dielectric properties. To this end, most current SAR systems are now offering increased information content by achieving diversity in polarimetry, frequency, observation angle (interferometry and tomography), temporal data and together with enhanced image resolution. It is clear that backscattering from complex targets is heavily influenced both of these target and radar parameters thereby preventing the derivation of definite conclusions in many instances. Ground-based (GB) radars allow a simple and practical way of understanding and predicting the backscattering mechanisms which would be helpful for validation and research of spaceborne and airborne SAR applications. For this purpose, various ground-based scatterometers [1–3], imaging radars (GB-SAR) [4] and interferometers [5] have been studied.

In an attempt to better understand this complex scattering mechanism, we are concerned with the experimental assessment of polarimetric L-band backscattering of a typical land surface and canonical targets through GB-SAR data. The outline of this paper is as follows: Section 2 explains the experimental scenario of our polarimetric GB-SAR imaging system. The measured images and their polarimetric analysis results are presented in Section 3. Concluding remarks are given in the last section.

2. EXPERIMENTAL SCENARIO

We adopted the two-dimensional (2-D) quasi-monostatic GB-SAR imaging geometry shown in Fig. 1(a). The radar platform was located at a certain height h and moved along the cross-range axis for a scanning length of L with azimuth steps of Δx resulting in atypical strip-map SAR collection. The transmitter (TX) and receiver (RX) antennas were slanted with an incidence angle β' from the vertical direction. The β and α angles represent local incidence angle and depression angle, respectively within the desired imaging area denoted with $D(x, y)$. The implemented SAR system is shown in Fig. 1(b). The setup consisted of a vector network analyzer (VNA) with stepped frequency continuous wave radar operation with a frequency range from 300 kHz to 8.5 GHz, an RF amplifier of 1 Watt power, Vivaldi horn antennas functioning between 300 MHz and 3300 MHz, a laptop and a stepper motor mechanism for moving the platform.

3. MEASUREMENT RESULTS

The GB-SAR measurements were carried out on a building's roof terrace that lies 14 m above the ground level. The backscattering data were collected for a frequency span of 1.5 GHz to 3 GHz with 801 sampling points and a synthetic aperture length of 14.7 m with 10 cm steps. The picture in Fig. 2 shows the test scene as seen from the radar location. The scene was composed of a series of trees, a pave road, a gazebo, plants and add-on canonical targets such as five trihedral corner

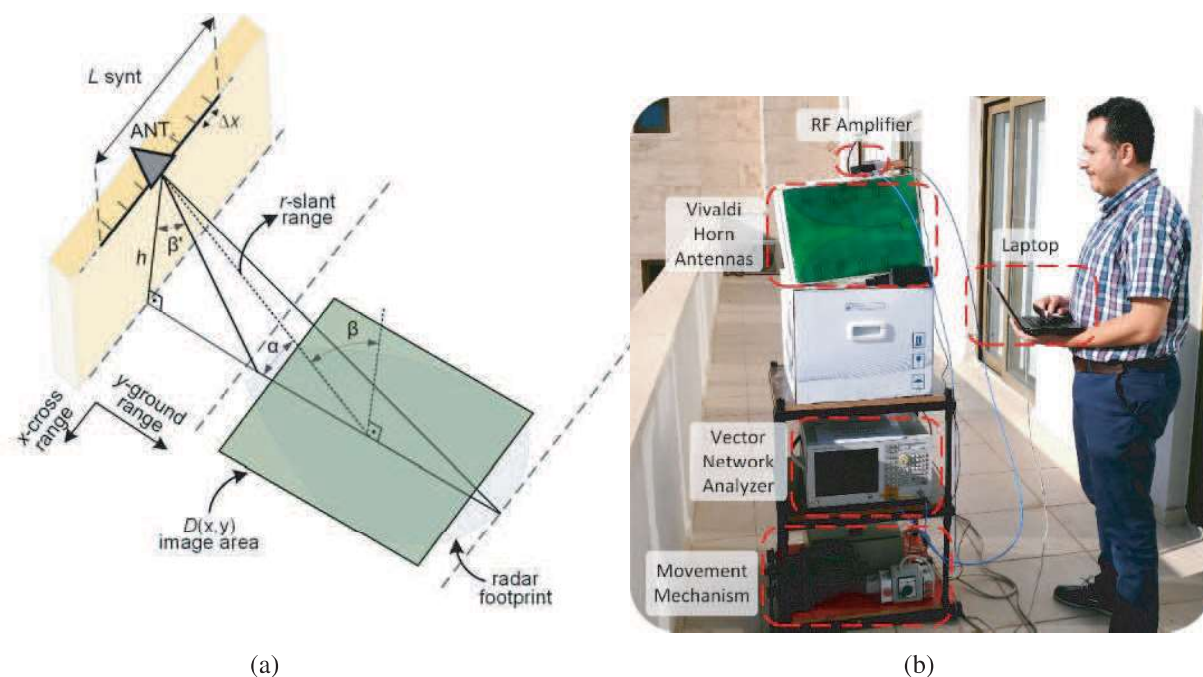


Figure 1: (a) 2-D GB-SAR imaging geometry, (b) experimental measurement-setup.

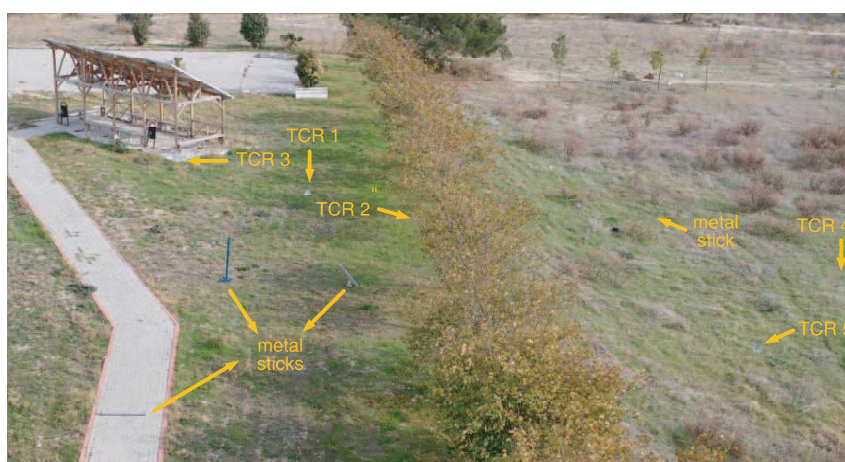


Figure 2: Photograph of the test field with description of the add-on targets.

reflectors (TCR) and four metal sticks. Two of the metal sticks were oriented at about 45° and the other two were placed horizontally and vertically as seen from the figure. The radar echo of the test scene was received for three polarization channels (HH , VV and HV). After applying the near-field backprojection algorithm, the focused SAR images were obtained as shown in Fig. 3. As it can be deduced from the figure, the layout of the terrain and especially all canonical targets can be predominantly seen from the co-polar images. Besides, natural distributed areas, complex-shaped gazebo and tilted metal sticks all give rise to depolarization as understood from their strong responses in cross-polar image. Moreover, we applied the Pauli decomposition to the measured data to discriminate the scattering mechanisms. In this decomposition, the scattering matrix $S_{(\hat{u}_H, \hat{u}_V)}$ defined as,

$$S_{(\hat{u}_H, \hat{u}_V)} = \begin{bmatrix} S_{HH} & S_{HV} \\ S_{VH} & S_{VV} \end{bmatrix} \quad (1)$$

is converted to target scattering vector $\bar{k}_{P(\hat{a}_H, \hat{a}_V)}$ with the following equation

$$\bar{k}_{P(\hat{a}_H, \hat{a}_V)} = \begin{bmatrix} k_1 \\ k_2 \\ k_3 \end{bmatrix} = \frac{1}{\sqrt{2}} \begin{bmatrix} S_{HH} + S_{VV} \\ 2S_{HV} \\ S_{VV} - S_{HH} \end{bmatrix} \quad (2)$$

The k_1 component represents single or odd-bounce scattering caused by a scatterer of a plate, trihedral or sphere and is coded as blue color using RGB color space. Second component k_2 of coherent scattering vector represents volume scattering contribution like forest cover and corresponds to the scattering matrix of a 45° oriented dipole. The last component k_3 stands for the contribution of a dihedral scattering which produces double or even bounce scattering mechanism [6]. Green and red colors in Pauli images are assigned with k_2 and k_3 components, respectively. Fig. 4(a) shows the Pauli decomposition image of our polarimetric GB-SAR data. Firstly, though TCRs are expected to show up in blue color tones, their features are seen as magenta colortones (blue + red) due to the interaction of the electromagnetic wave with non-ideal ground conditions and also the lack of full-polarimetric calibration. Secondly, tilted metal sticks, complex-shaped structures and tree regions all experience volume scattering phenomena; so they appear in green color tones in the image. Lastly, horizontal metal stick is observed to produce double-bounce scattering because of the dihedral structure formed with ground-plane at this operated wavelength. Figs. 4(b) and 4(c) show total power (span) and orientation angle (i.e., beta) images, respectively. All the targets oriented in azimuth direction, including the two 45° oriented metal sticks, the complex gazebo structure, the trees and other vegetation targets that lay on tilted surfaces can be readily distinguished from

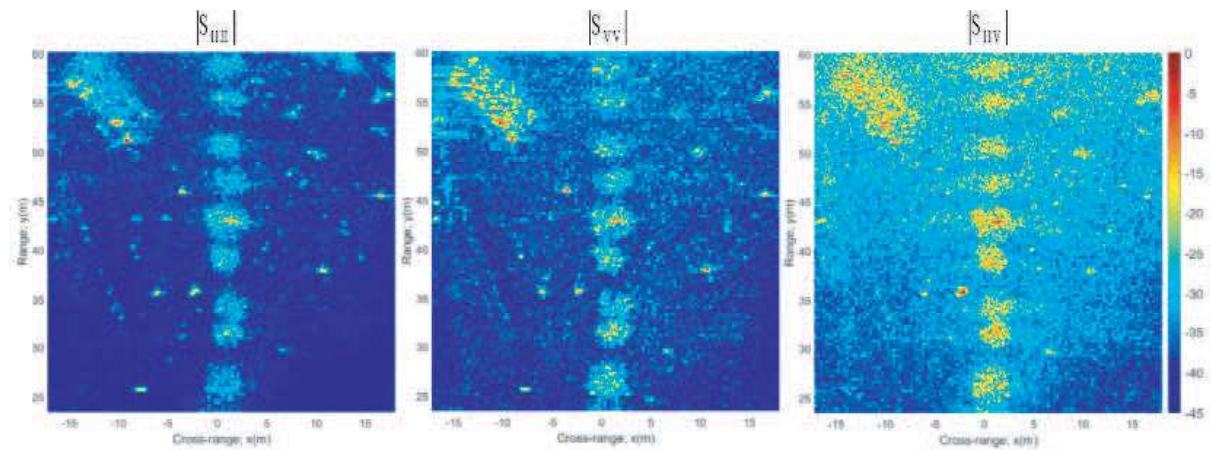


Figure 3: Back-projection based near-field GB-SAR imaging results.

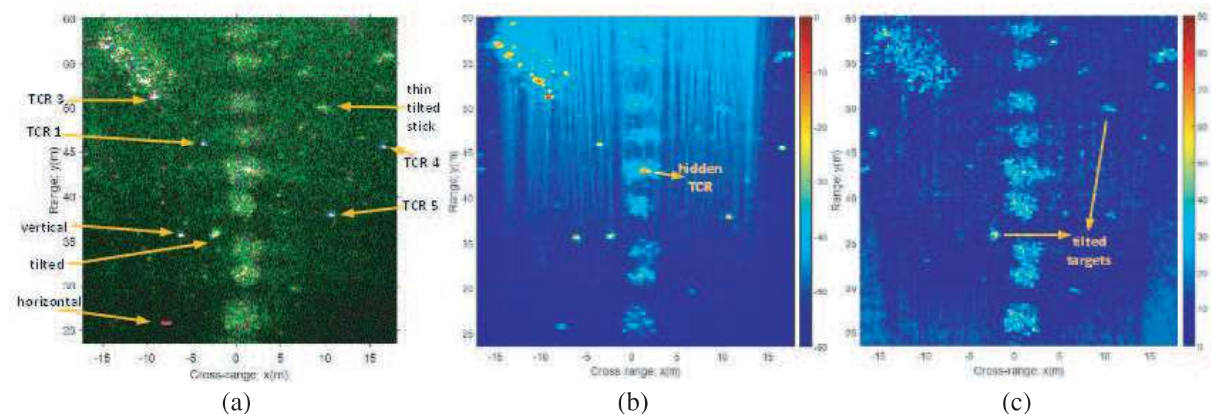


Figure 4: Polarimetric radar imaging analysis results: (a) The Pauli decomposition image using blue for surface, red for double-bounce and green for volume scattering. (b) Total power (span) image. (c) Orientation angle (beta) image.

the beta-angle image. Also, the span image indicates that the measured total backscattered powers are in good agreement with those predicted polarimetric backscattering signatures of natural and man-made targets.

4. CONCLUSION

We presented a proof-of-concept type study for the employment of polarimetric GB-SAR imaging technology. An experimental assessment of the polarimetric L-band backscattering of a typical terrain and man-made targets was made through GB-SAR data. The measurement set-up and the geometry were explained. We have shown that while co-polar (VV and HH) images are more sensitive to deterministic man-made objects such as corner reflectors and dipole-like targets, cross-polar (VH and HV) images mostly respond to natural scatterers such as trees, plants as well as to tilted and complex-shaped man-made targets, as expected. The Pauli, the span and the beta-angle images of the GB-SAR backscattering data provided satisfactorily efficient means to interpret the scattering mechanisms occurring within the scene.

REFERENCES

1. Albinet, C., P. Borderies, T. Koleck, F. Rocca, S. Tebaldini, L. Villard, T. Le Toan, A. Hamadi, and D. Ho Tong Minh, "TropiSCAT: A ground based polarimetric scatterometer experiment in tropical forests," *IEEE Journal of Selected Topics in Applied Earth Observations and Remote Sensing*, Vol. 5, No. 3, 1060–1066, 2012.
2. Lopez-Sanchez, J. M., J. David Ballester-Berman, and J. Fortuny-Guasch, "Indoor wide-band polarimetric measurements on maize plants: A study of the differential extinction coefficient," *IEEE Transactions on Geoscience and Remote Sensing*, Vol. 44, No. 4, 2006.
3. Ozdemir, C., *Inverse Synthetic Aperture Radar Imaging with MATLAB Algorithms*, John Wiley & Sons, 2012.
4. Penner, J. F. and D. G. Long, "Ground-based 3D radar imaging of trees using a 2D synthetic aperture," *Electronics*, Vol. 6, 11, 2017.
5. Nico, G., D. Leva, G. Antonello, and D. Tarchi, "Ground-based SAR interferometry for terrain mapping: Theory and sensitivity analysis," *IEEE Trans. Geosci. Remote Sens.*, Vol. 42, No. 6, 1344–1350, Jun. 2004.
6. Brunner, D., L. Bruzzone, A. Ferro, and A. Lemoine, "Analysis of the reliability of the double bounce scattering mechanism for detecting buildings in VHR SAR images," *2009 IEEE Radar Conference*, 1–6, Pasadena, CA, 2009.